Journal of Optoelectronics and Advanced Materials Vol. 7, No. 5, October 2005, p. 2353 - 2358

PROPERTIES OF HIGH-POROSITY SOL-GEL DERIVED INDIUM-TIN OXIDE FILMS

T. F. Stoica*, M. Gartner[a], T. Stoica, M. Losurdo[b], V.S. Teodorescu, M. G.Blanchin[c], M. Zaharescu[a]

National Institute of Materials Physics, P.O.B. Mg.7, Str. Atomistilor 105bis, 77125-Bucharest-Magurele, Romania
[a]Institute of Physical Chemistry of the Romanian Academy of Sciences, Splaiul Independentei 202, 77208-Bucharest, Romania
[b]Plasma Chemistry Research Center-CNR, via Orbona, 4 –70126 Bari, Italy
[c]Laboratoire de Physique de la Matiere Condensee et de Nanostructures, Universite Claude Bernard Lyon 1 $3 Boulevard du 11 novembre 1918, 69622 Villeurbanne Cedex, France

Indium-tin oxide (ITO) sol-gel films have been obtained with the void concentration up to 50%. The films are nanostructured with nanocrystals of In_2O_3:Sn and nanovoids. The information obtained from derivative thermo-gravimetry was used to design the annealing program for ITO film formation with a high void concentration. Multilayer films were obtained by successive deposition. The thickness of one layer was about 9 nm. By successive depositions, the void density of the film is reduced. Quantitative analysis of the void density has been performed by spectroscopic ellipsometry. The conductivity of the films can be varied in a large range by annealing in vacuum or in air, at temperature higher than 200 °C.

(Received August 29, 2005; accepted September 22, 2005)

Keywords: Sol-gel method, Indium-tin oxide, Thin films

1. Introduction

Indium oxide is a wide band gap material (3.3 eV), which can have a high optical transparency in the visible wavelength range and a high conductivity due to the oxygen vacancies, acting as donor states [1]. To increase the conductivity up to the metallic conductivity (10^3-10^4 $\Omega^{-1}cm^{-1}$), a solid solution of indium-thin oxide (ITO) with a few percent of Sn is used. The area of applicability of these transparent conductive (TCO) films is very large: optoelectronics, antistatic coatings and infrared reflectors [2,3]. The properties of ITO films depend very much on deposition and annealing methods [4-7]. We have investigated different methods to obtain ITO films suitable for different kinds of applications [8,9]. A special attention was paid to the sol-gel film preparation by alkoxide route [10-13]. Sol-gel method offers a very good control of the composition and of the film properties by variation of the internal film structure. Films with nano-crystals and nano-pores of different density and size can be obtained.

In this paper we investigate sol-gel ITO films with the aim at controlling the porosity of the films in a wide range, and its consequences on electrical and optical properties.

2. Experimental details

Indium and tin propoxides $In(OC_3H_7)_3$ and $Sn(OC_3H_7)_4$ were dissolved in isopropylalcohol (PrOH) to form ITO sol-gel solution. Different sol-gel solution indicated as S1..S9 were used for

* Corresponding author: tfstoica@infim.ro

deposition of ITO films with different void density. The composition of the solutions used for films deposition is presented in Table1.

The sol was deposited by spin coating method followed by annealing at different temperature steps up to 550 °C to form ITO films. The annealing program for the film formation was established, based on the results obtained by derivative thermogravimetry-thermal analysis (DTG-DTA), made by using a MOM – Q derivatograph. Multilayer films were obtained by successive depositions. Spectroscopic Ellipsometry (SE), X-ray Photoelectron Spectroscopy (XPS), Transmission Electron Microscopy (TEM) and Atomic Force Microscopy (AFM) were used for film characterization. Electrical measurements were performed in a cryostat in the temperature range 10 – 300 K using a Keithley source-measure unit. The annealing at higher temperatures were performed in a vacuum chamber or in air.

Table 1. The composition of the solutions used for films deposition.

Solut. No.	$In(OC_3H_7)_3$ (mol/l)	Solvent	Sn precursor	Sn/In (%)	pH	Complex.	Complex./ In (molar ratio)
S1	0.25	PrOH	$Sn(CH_3)_4$	10.7	3.6	oleic acid	0.69
S2	0.43	PrOH	$SnClH_{27}C_{12}$	15.5	2.2	oleic acid	0.74
S3	0.41	PrOH	$Sn(OC_3H_7)_4$	3.9	3..3	oleic acid	0.80
S7	0.45	PrOH	$Sn(OC_3H_7)_4$	5.0	5.7	TEA	0.37
S9	0.38	EtOH	$Sn(OC_3H_7)_4$	2.0	5.3	TEA	0.26

$In(PrO)_3$ = $In(OC_3H_7)_3$; $Sn(PrO)_4$=$Sn(OC_3H_7)_4$; PrOH= isopropylalcohol; EtOH = ethanol; Complex.= Complexing agents: oleic acid or TEA=triethanolamine.

3. Results and discussions

Information about reaction temperatures in ITO gel obtained from derivative thermogravimetry (DTG) studies are very important for setting the annealing steps for film formation. After a massive H_2O evaporation, the decomposition and burning out of the organic components of the used precursors take place at about 340 °C [14]. The annealing steps and the temperature ramp in the low temperature range are crucial for controlling void density and achieving the desired chemical composition of ITO films. Decomposition of ITO takes place at temperatures higher than 600°C, by oxygen effusion. In this paper the annealing program for the film formation was designed to obtain a high percent of voids. Annealing above 200 °C results in partial effusion of oxygen, depending on the oxidant or reducing character of the annealing atmosphere. For high density of voids and high porosity, films are more sensitive to the annealing atmosphere, suitable for gas sensors. The samples were obtained by 1 to 7 successive depositions, using the solutions described in Tab. 1.

The film composition has been investigated by XPS measurements. The high resolution $In3d_{5/2}$, $Sn3d_{5/2}$ and O1s peaks are shown in Fig. 1a,b and c, respectively.

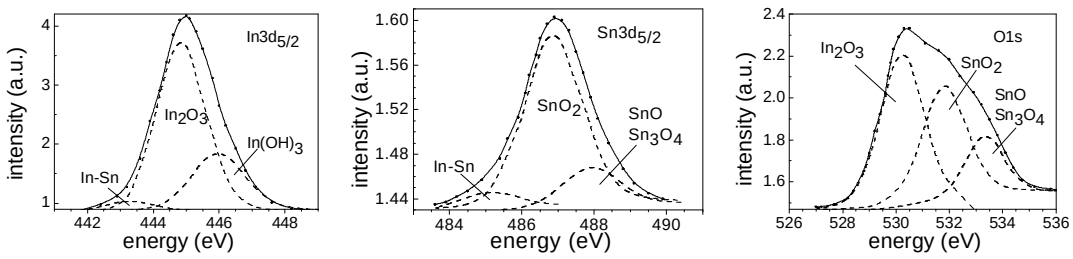

a b c

Fig. 1. High resolution XPS peaks: a)- $In3d_{5/2}$, b)- $Sn3d_{5/2}$,and c)- O1s.

The peak deconvolutions show different contributions assigned in Fig. 1 to different bonds [15]. The above peaks present the evidence of In_2O_3 and SnO_2 formation in a solid solution. Moreover, a O/(In+Sn) ratio of approximately 1.8 has been found. This value is higher than that of

commercial sputtering-deposited films (usually smaller than 1.7). This is in agreement with the lower conductivity and higher void density of sol-gel ITO films, corresponding to an oxygen vacancy density lower than that of films from other techniques.

Internal and surface morphology have been studied by XTEM and AFM, respectively. High resolution XTEM images show an internal structure corresponding to nanocrystals and nanovoids with the size of the order of 20 nm [16]. The nanocrystals shown by high-resolution TEM have a crystalline network of In_2O_3, and segregation of SnO_2 has not been detected. This corresponds to a solid solution character of the sol-gel ITO films, in agreement with the XPS results.

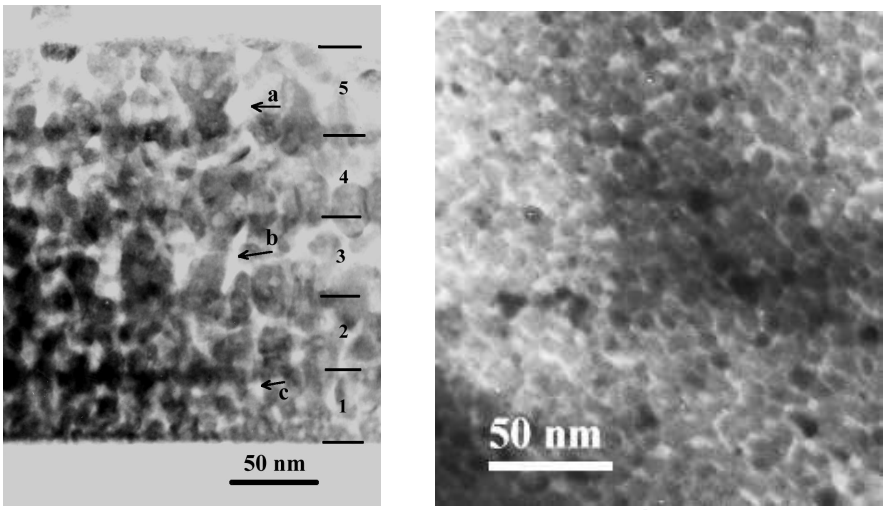

a b

Fig. 2 a)- Cross sectionTEM image of the 5-layer (5 x 50 nm) ITO film. Different morphology of voids are identified: big void in the last deposited layer (label a); needle like void in the intermediate layer (label b); small void in the first deposited layer (label c). b)- Plan view TEM image of a 9 nm thick ITO monolayer. There are a high density of small voids (3 to 5 nm large and 10 to 20 nm long). These voids are situated at the boundaries of the ITO nanocrystallites.

In Fig. 2a, a cross section TEM image of a multilayer sol-gel ITO films is shown. For this sample, a different solution than the solutions in Table I was used to obtain a relative thick layer for one deposition, for better observation of void evolution effect due to successive depositions. The single layer has in this case a thickness of about 50 nm.

The void dimension decreases from the last to the first deposited layer (voids labeled a, b, c in Fig. 2a). Each interface between successive ITO layers is more dense like the average ITO layer density. It can be also seen that the void density is relatively lower within the top layers, while the dimension of the voids is much bigger. One can suppose that the successive depositions fill partially the pores in the already deposited layers. This pore filling process increases slowly the void density because the big voids are only partially filled and divided in several smaller ones. So, the void dimension decreases drastically for previously deposited layers, but the void density increases as well as the mean value of the ITO layer density.

We can conclude that the small voids in the first deposited layers (1) are isolated ones, but big voids in the last deposited layer (5) are connected forming a labyrinth of pores in the layer.

Fig. 2b presents a plan view TEM image of a 9 nm thick ITO monolayer. This image reveals a very high density of voids, which appear al the limit of the ITO nanograins. The voids are 3 to 5 nm large and can be as long as 20 nm. The grains have between 5 and 10 nm in size. The film grains touch each other in a few points. In between ITO grains, there are in majority void. The 9 nm thick sol-gel one-deposition film is practically formed by a monolayer of ITO nanograins. The density of the ITO layer can be estimated at 40- 50% if we consider the model of the monolayer ITO nanograins.

Comparing the two images in Fig. 2, we can conclude that the density and the size of the voids present in the ITO sol-gel films are very different, function of the thickness of each deposited layer and the order of the deposited layer in the case of multilayer films.

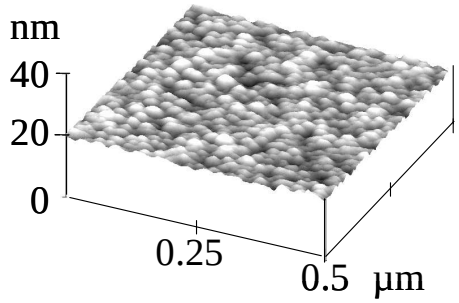

Fig. 3. Surface morphology revealed by AFM imaging of a sol-gel ITO multilayer film.

In spite of a high porosity of the films revealed by TEM images, the films are relatively smooth as can be seen in the AFM image of Fig. 3. This is because the voids and crystallites are however of sizes of 20-30 nm. The nanocrystals revealed by cross section XTEM results in small domes of the AFM surface topography in Fig. 3 in agreement with the data in Ref. [17].

The density of voids has been quantitatively evaluated using spectral ellipsometry. Fig.4a shows the void density is shown as function of the number of the successive deposited layer for samples obtained using the different solutions described in Tab. I. The void density is evaluated as a volume ratio.

The void density can reach a value of 50% and decreases with the number of layers as can be seen in Fig. 4a, in agreement with the results of XTEM results. The optical properties strongly depend on void density. Spectral dependence of the refractive index and of the absorption coefficient determined by modeling of SE data correlates very well with the void density. The refractive index for the same samples of Fig. 4a is shown in Fig. 4b as a function of void density, for the wavelength of 357 nm. The refractive index varies in a very wide range from 1.9, close to the ITO bulk value, to 1.5 for very spongy films.

From spectral ellipsometric data, the thickness can also be estimated. For the layer prepared with the solution S1-S3, a mean value of about 9 nm/layer for the samples in Fig. 4 has been obtained, in agreement with interferometric microscopy and AFM of samples with patterning obtained by chemical etching. Such a small thickness of the one-deposition layers can explain the relative strong dependence of the void density vs. number of layer, because a very thin porous layer can be easily influenced by the next deposition.

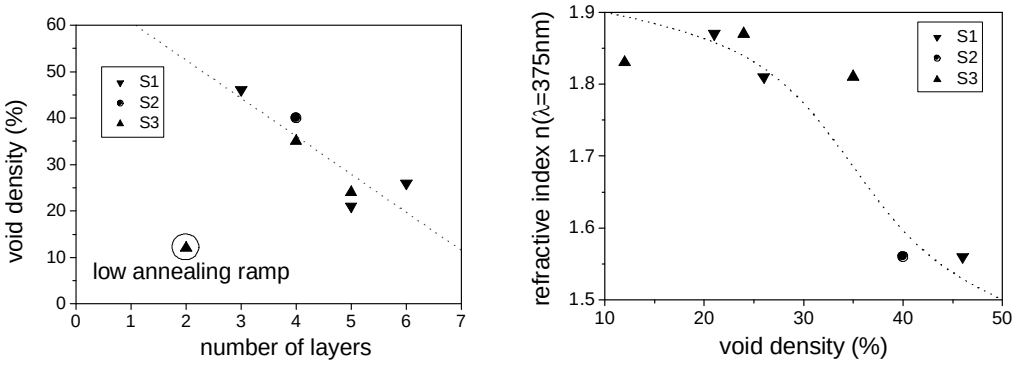

a b

Fig. 4 Void density as a function of the number of layers (a) and refractive index at the wavelength of 378 nm vs. void density (b). Results are obtained by analysis of the ellipsometric measurements. One sample with low density of voids (see the specific point in (a)) was obtained with a lower annealing ramp.

Electrical conductivity is very sensitive to film nanostructure, not only because this can influence the mobility of the carriers, but also their density. Modification of the electrical conductivity is obtained by annealing in different atmospheres. The annealing effects in ITO films are mainly related to the oxygen vacancies, which act as donor states. An oxidant atmosphere can reduce the oxygen vacancy density and, hence, the carrier density. The sol-gel films can be obtained with a high density of voids, as shown above. The high void density corresponds to a high porosity of the films, which results in a sensitivity to the annealing atmosphere and temperature of sol-gel ITO films higher than that of films obtained by other techniques.

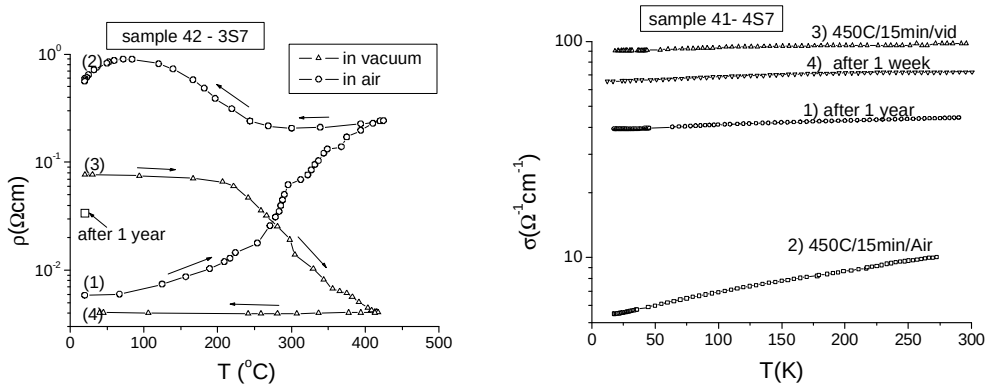

Fig. 5 a)- Effects of annealing in vacuum and air on the resistance of a sample consisting of deposition of 3 successive layer s. b)- temperature dependence in the range 10-300K of the conductivity for different states of a same with 4 successive depositions using the same solution S7 as for the sample in (a).

Indeed, the resistance can be varied orders of magnitude by annealing in vacuum or in air. The variation of the film resistance during different annealing processes is shown in Fig. 5a for a film with 3 successive layers. Different states of the sample at room temperature are labeled from 1 to 4. Arrows indicate the direction of temperature variation. The resistance of the sample increases by annealing in air starting from state 1, and remains of high value by cooling down the sample (state 2). After a few days at room temperature in air, the resistance has decreased to the state 3. By annealing in vacuum, the sample becomes again of low resistance (state 4). After one year in air at room temperature, the resistance was changed to an intermediary value between those obtained after annealing in air and vacuum. The annealing effects can be understood by the oxygen vacancy evolution: while the annealing in air produces by oxidation a reduction of oxygen vacancy density, the vacuum annealing increases this density [13]. The annealing effect becomes significant for temperatures higher than 200 °C, generally obtained for ITO films [10], but more pronounced in the case of very porous sol-gel films.

The temperature dependence of the conductivity at low temperatures in the range 10 - 300 K is shown in Fig. 5b for different states of the sample: 1- after one year aging in air; 2-after air annealing at 450 °C; 3- after vacuum annealing at 450 °C; and finally the state 4- after one week in air at room temperature. A conductivity as high as 10^2 $\Omega^{-1}cm^{-1}$ is achieved after annealing in vacuum. This is a quite high conductivity for thin (~30nm) nanostructured ITO films. The film conductivity is almost constant within the all range of the measurement temperature 10-300 K, except for the low-conductivity state after annealing in air, for which small activation energy is observed.

4. Conclusions

ITO sol-gel multilayer films with the void density varied in a wide range have been obtained. TEM and AFM revealed the nanostructured character of the sol-gel films. DTG analysis has been used to optimize the formation of films with high void density. Spectral ellipsometric studies have been used for quantitative evaluation of the void density. The single-deposition layers have the thickness of ~9 nm and a porosity of 50%. Optical and electrical properties are well correlated with the void density. A high electrical sensitivity to different annealing atmospheres was observed.

References

[1] P. Mohan Babu, B. Radhakhrishna, G. Venkata Rao, P. Sreedhara Reddy, S. Uthanna, J. Optoelectron. Adv. Mater. **6**(1), 205 (2004).
[2] A. Arnaud, J. Non-Cryst. Solids **218**, 12 (1997).
[3] B. G. Lewis, D. C. Paine, M. R. S. Bull. **25**(8), 22 (2000).
[4] M. A. Martinez, J. Herrero, M. T. Gutierez, Thin Solid Films **348**, 273 (1999).
[5] N. G. Patel, P. D. Patel, V. S. Vaishnav, Sensors and Actuators **B 96**, 180 (2003).
[6] A. Nakasa, M. Adachi, E. Suzuki, H. Usami, H. Fujimatsu, T. Ohashi, S. Yamada,Y. Taniguchi, Thin Solid Films **484**, 272 (2005).
[7] R. B. H. Tahar, T. Ban, Y. Ohya, Y. Takahashi , J. Appl. Phys. **83**, 2631 (1998).
[8] M. J. Alam, D. C. Cameron, Thin Solid Films **420-421,** 76 (2002).
[9] Z. Jiao, M. Wu, J. Gu, X. Sun, Sensors and Actuators **B 94**, 216 (2003).
[10] Y. Takahashi, H. Hayashi, Y. Ohya, Mat. Res. Soc. Proc. **271**, 401 (1992).
[11] M. Toki, M. Aizawa, J. of Sol-Gel Science and Tehnology **8**, 717 (1997).
[12] H. Tomonaga, T. Morimoto, Thin Solid Films **392**, 243 (2001).
[13] M. Raileanu, M. Crisan, C. Petrache, D. Crisan, M. Zaharescu, J. Optoelectron. Adv. Mater. **5**(3), 693 (2003).
[14] T. F.Stoica, T. A. Stoica, M. Zaharescu, M. Popescu, F. Sava, N. Popescu-Pogrion, L. Frunza, J. Optoelectron. Adv. Mater. **2**, 684 (2000).
[15] F. Moulder, W. F. Stickle, P. E. Sobol, K. D. Bomben, "Handbook of X-ray Photoelectron Spectroscopy", Ed. J. Chastain, Perkin-Elmer Corporation Physical Electronics Division, 1992.
[16] T. F. Stoica, V. S. Teodorescu, M. G. Blanchin, T. A. Stoica, M. Gartner, M. Losurdo, M. Zaharescu, Materials Science & Engineering B **101**, 222 (2003).
[17] D. Gallagher, F. Scanlan, R. Houriet, H. J. Mathieu, T. A. Ring, J. Mater. Res. **8**(12), 3135 (1993).